Research Square

Preprints are preliminary reports that have not undergone peer review.
They should not be considered conclusive, used to inform clinical practice,
or referenced by the media as validated information.

Stationary and Mobile Storage for Base Stations: Joint Reserve and Energy Management

Mohammad Reza Jokar

mohammad.jokar@polito.it

Politecnico di Torino

Greta Vallero

Politecnico di Torino

Daniela Renga

Politecnico di Torino

Michela Meo

Politecnico di Torino

Research Article

Keywords: Base stations, Electric vehicles, Stationary batteries, Reserve sharing, Energy arbitrage, Battery degradation, Power outages

Posted Date: November 10th, 2026

DOI: https://doi.org/10.21203/rs.3.rs-11322863/v1

License: This work is licensed under a Creative Commons Attribution 4.0 International License.
Read Full License

Additional Declarations: No competing interests reported.

Stationary and Mobile Storage for Base Stations: Joint Reserve and Energy Management

Mohammad Reza Jokar[1*], Greta Vallero[1], Daniela Renga[1], Michela Meo[1]

[1*] Department of Electronics and Telecommunications, Politecnico di Torino, Corso Duca degli Abruzzi 24, Turin, 10129, Italy .

*Corresponding author(s). E-mail(s): mohammad.jokar@polito.it;

Abstract

Base-station backup batteries are kept at high state of charge to support communication during grid outages, restricting their use for electricity-price arbitrage during normal operation. This study examines whether connected electric vehicles (EVs) can provide temporary backup reserve and release stationary storage for economic dispatch. A degradation-aware framework accounts for EV energy, discharge power, departure times, and owner compensation, while a causal outage controller prioritizes served traffic without knowing grid-restoration time or future EV arrivals. Paired comparisons separate EV backup, reserve release, and direct EV dispatch. For one annual load and fleet scenario with a 10 kWh stationary battery and 2024 prices, joint dispatch reduces total normal-operation cost by 2.91% in Italy and 8.36% in the Netherlands relative to stationary standby. Almost all savings arise from reserve-enabled stationary dispatch. In sampled 24 h outages, mean retained traffic increases from 23.12% to approximately 84.5%; receding-horizon control also gains about 26 percentage points over one-step control with identical initial resources and information. Reduced calendar aging is offset by additional cycling. These results assume existing compatible bidirectional infrastructure and do not establish new-installation payback or adequate owner incentives.

Keywords: Base stations, Electric vehicles, Stationary batteries, Reserve sharing, Energy arbitrage, Battery degradation, Power outages

1 Introduction

A backup battery has a clear purpose at a cellular base station (BS): it keeps the site operating when the electricity grid fails. In standby operation, the battery is kept at a high state of charge (SOC), ready for an interruption that may occur at any time. This readiness matters, but it also limits how the installed battery can be used while the grid is available. At sites where outages are infrequent, the battery can remain largely unused for long periods. Outage frequency and duration nevertheless depend on the local supply conditions, as illustrated by distribution-network reliability statistics [1]. Energy that could supply the site during expensive hours therefore remains reserved for backup. Research on BS battery dispatch has investigated how this capacity can support other functions while respecting communication and backup requirements [2, 3].

Using this capacity for economic operation, however, is not a simple price-arbitrage problem. Battery dispatch affects both degradation and the energy retained for backup. Maintaining a high SOC preserves outage readiness but can accelerate calendar aging, whose dependence on SOC and temperature has been characterized for stationary-battery cells [4, 5]. Conversely, operating at a lower average SOC may reduce calendar aging, but additional charge–discharge cycles introduce cycling degradation and may leave less energy available when an outage occurs. The economic value of battery operation therefore depends on electricity savings, degradation, and backup availability, rather than on the electricity-price spread alone.

One way to relax this trade-off is to complement the stationary battery with energy from parked electric vehicles (EVs), accessed through bidirectional charging. When participating EVs are connected, part of their available energy can temporarily contribute to the backup reserve, allowing the stationary battery to operate more flexibly during grid-connected periods. In the architecture considered here, EVs supplement the stationary battery rather than replace it: their availability depends on vehicle presence. We refer to the stationary battery as *persistent storage* and the connected EV batteries as *temporary storage*.

This distinction gives EVs two potential sources of value during normal operation. They can discharge when electricity prices justify the cost of using their batteries, or remain connected and contribute to the backup reserve. In the second case, an EV may deliver no energy during normal operation, yet its presence can allow the stationary battery to supply the site during expensive hours. During an outage, EV energy may instead help sustain communication service. These benefits accrue to different parties: lower site costs do not necessarily imply substantial earnings for EV owners.

EV support is limited by the vehicle's minimum SOC, charger power, connection time, and the compensation required for battery use [6, 7]. Once a vehicle leaves, its remaining energy is no longer accessible to the BS. During an outage, using some of that energy before departure may preserve stationary energy for later, but this decision also depends on the load, power limits, and battery costs. Releasing stationary reserve during normal operation may reduce costs while weakening backup performance in some outage cases; whether the trade-off is worthwhile must be evaluated rather than assumed.

This article extends our EuCNC & 6G Summit paper [8], which introduced on-site EV reserve as a way to increase stationary-battery utilization and included battery aging and a conditional EV reserve payment. The present study develops this concept further by distinguishing EV reserve provision from direct energy delivery, accounting separately for replacement energy, EV degradation, and owner margin, and coordinating storage and radio operation during outages without knowledge of the actual grid-restoration time. A year-long evaluation examines the operating value of this coordination with existing compatible bidirectional charging infrastructure. A separate cost screen considers the boundary for new infrastructure, without establishing installation payback.

During grid-connected operation, a rolling mixed-integer linear program schedules storage use based on energy costs, battery wear, and EV-owner payments. When no EV reserve is available, the stationary battery retains its standby energy. When connected EVs contribute to the reserve, part of that requirement can be shifted away from the site battery, subject to SOC, power, and connection-time constraints. During an outage, a receding-horizon controller first prioritizes served traffic and then minimizes operating cost. It coordinates the stationary battery, the currently connected EVs, and the active radio carriers. Outage decisions use current observations and forecasts, without knowledge of the actual restoration time, future EV arrivals, or future traffic realizations. Normal-operation scheduling instead uses the supplied demand path and scheduled sessions, so its economic comparison is conditional on that information.

The evaluation combines an annual demand scenario resampled from a measured single-site BS trace, generated EV-parking sessions, and 2024 day-ahead price series for Italy and the Netherlands from the ENTSO-E Transparency Platform [9]. Public office-parking data from Utrecht [10] provide an empirical reference for the parking setting; the simulations use parametric sessions rather than replaying or fitting the original records. EV battery states and participation levels are scenario assumptions. The two price profiles are applied to the same site and vehicle scenarios to provide a controlled comparison of electricity-market conditions, rather than a comparison of two measured national deployments. Outages of up to 24 h include cases in which vehicles arrive or depart before grid power returns.

The main contributions of the journal extension are:

- An extended storage-coordination model that combines persistent stationary storage and temporary EV storage with individual connection times, SOC limits, charger constraints, battery aging, and explicit EV-owner compensation. It distinguishes the use of EVs as reserve from their direct energy delivery during normal operation.
- A causal outage controller that jointly manages storage dispatch and carrier-level operation. Outage cases start from the battery states produced during normal operation. Matched-state comparisons examine outage support at common initial stationary energy, and a one-step benchmark assesses planning under the same initial conditions and available information.
- A year-long evaluation that separates the economic and operational effects of EV-enabled stationary-battery use, direct EV dispatch, and emergency support under Italian and Dutch day-ahead price profiles. Paired policy comparisons and sampled outage events assess site savings, owner profit, and served traffic. Outage-frequency

sensitivity provides an economic screening analysis, rather than a chronological simulation of repeated outages and recovery.

Section 2 reviews the relevant literature. Sections 3 and 4 present the system model and control framework, while Section 5 describes the evaluation setup. Results, deployment implications, limitations, and conclusions are presented in Sections 6–8.

2 Related Work

Using EVs as temporary backup at a BS draws on three areas of research: stationary-battery operation, EV availability and compensation, and communication service during power outages. The following review connects these areas and identifies the scope of the present extension.

2.1 Stationary batteries and base-station operation

Yong et al. [2] evaluate the dispatchable capacity of BS backup batteries, examining their use beyond standby while retaining backup reliability requirements. Gholipoor et al. [3] coordinate cellular-network storage and communication resources for frequency regulation, including SOC and cycling constraints and an explicit battery degradation cost. Cabrera-Tobar et al. [11] develop adaptive model-predictive energy management for a BS supplied by a renewable-based microgrid, considering grid-connected and outage operation. These studies establish that telecom batteries can support functions beyond backup. Their focus differs from sharing the site battery's standby reserve with EVs whose energy is available only during their connection intervals.

Communication demand also affects how long backup energy can sustain service. Zheng et al. [12] study battery configuration, demand transfer, and BS sleep decisions under uncertain interruption duration using a two-stage stochastic formulation. Our setting instead considers an already installed battery at a single site, with outage decisions updated as traffic and connected EV resources change. Carrier-level operation changes the site's demand, while storage coordination determines how that demand is supplied.

The evaluation of battery use must account for degradation as well as energy cost. Naumann et al. [4] characterize calendar aging under different SOC and temperature conditions for a lithium iron phosphate (LFP)/graphite cell. Xu et al. [13] incorporate a piecewise-linear cycle-aging cost into electricity-market dispatch. Collath et al. [5] investigate aging-aware stationary-battery operation and lifetime profitability, considering calendar and cycling degradation. These works motivate evaluating both mechanisms when releasing standby reserve: reducing average SOC does not, by itself, establish that total wear or operating cost will decrease.

2.2 EV availability and the cost of participation

EV availability is shaped by arrivals and departures. Truong and Le [14] consider random connection times, battery degradation, and EV charging in building energy management. Thrän et al. [15] forecast aggregate EV power and energy bounds and use stochastic model-predictive control for reserve provision, examining how fleet size

affects predictability. These studies show why EV flexibility must be described by both available energy and its duration of access. At a site with only a few charging ports, a single departure can remove a substantial share of the temporary reserve. The Utrecht office-parking dataset [10] provides recorded charging sessions for studying connection patterns, but does not establish the SOC or willingness to provide backup of the vehicles modeled here.

Participation also has an economic cost. Leippi et al. [6] study employee EVs in industrial demand response and compensate owners through free charging while accounting for degradation. Sagaria et al. [7] analyze the degradation associated with vehicle-to-grid (V2G) operation and estimate compensation for the resulting owner costs. These studies motivate evaluating site savings together with the costs borne by vehicle owners. Our model accounts separately for replacement energy, incremental degradation, and an agreed owner margin. The compensation rule is an assumed contract, not an empirically established model of owner participation.

2.3 EV support during outages and the present extension

Ayaz et al. [16] study energy exchange between EVs and BSs in a disaster-affected region. Their digital-twin and reinforcement-learning framework matches energy buyers and sellers while representing power disruption and blocked routes through Markov models. It includes battery degradation and economic utility terms. This work addresses whether vehicles can reach suitable BSs and exchange energy after a disaster. Our study instead considers vehicles connected at the same site and examines how their temporary reserve affects stationary-battery use before an outage and service delivery during it.

Our conference paper [8] already considered EV-enabled reserve release, probabilistic vehicle connection intervals, stationary battery aging, and a conditional payment for EV reserve. These elements are the starting point of the extension.

Table 1 summarizes selected modeling features. *BS control* covers optimized site-energy or radio-resource decisions; *EV timing* covers connected availability or arrival/departure constraints. *Reserve release* specifically means using EV backup availability to relax stationary standby reserve during normal operation. *Wear cost* requires an explicit degradation cost, and *owner costs* cover payments or utility associated with EV participation. *Outage control* denotes a dedicated control strategy for operation during grid outages; this column does not establish whether future restoration times are known. The table compares scope, not performance.

Together, these studies provide models for storage dispatch, EV flexibility, participation costs, and emergency energy exchange. The question addressed here is how these elements interact at a BS when temporary EV reserve permits greater use of the persistent battery.

Table 1 Selected modeling features of representative studies.

Study	BS control	EV timing	Reserve release	Wear cost	Owner costs	Outage control
Gholipoor et al. [3]	✓	—	—	✓	—	—
Truong and Le [14]	—	✓	—	✓	—	—
Thrän et al. [15]	—	✓	—	—	—	—
Leippi et al. [6]	—	✓	—	✓	✓	—
Ayaz et al. [16]	✓	○[a]	—	✓	✓	✓
Jokar et al. [8] (conference)	✓	✓	✓	✓	○[b]	✓
Present work	✓	✓	✓	✓	✓	✓

✓: explicit treatment; ○: limited treatment; —: outside the scope defined above. [a]Vehicle reachability rather than parked-session departure constraints. [b]Conditional reserve payment without separate replacement-energy, EV-degradation, and owner-margin components.

3 System Model and Information Structure

3.1 Site architecture and operating regimes

We consider a grid-connected cellular BS equipped with an operator-owned battery energy storage system (BESS) and existing bidirectional EV charging ports. The grid, stationary battery, and connected vehicles supply a common site bus, as shown in Fig. 1. Electricity export and energy exchange with neighboring BSs are excluded. Compatible vehicles, converters, and equipment for islanded operation are assumed. Switching transients and electrical protection are outside the scope of the scheduling model.

The stationary battery remains at the site, whereas EV energy is accessible only while a vehicle is connected. We refer to these resources as persistent and temporary storage, respectively. Persistent availability does not imply unlimited stored energy. During normal operation, the site serves all offered traffic and schedules storage use subject to energy costs and a backup-reserve requirement. During an outage, grid import stops and the controller prioritizes carried traffic before minimizing the cost of supplying it. A connected EV may supply the site directly or charge the BESS, retaining some energy at the site after the vehicle departs.

Panel (a) shows the energy connections and control interface. Panel (b) illustrates how access to stationary and vehicle storage differs over time. The grid-switch labels indicate supply availability; the variable g_t introduced below denotes imported power.

3.2 Radio service and energy balance

Time is divided into intervals of duration Δt hours. Normal operation spans N intervals, indexed by $t = 0, \ldots, N-1$, with storage states defined at boundaries $t = 0, \ldots, N$. Full-service site power and offered traffic rate are ℓ_t^{full} and q_t^{full}, respectively. During an outage, the controller selects one operating mode m from the feasible set $\mathcal{M}_t$:

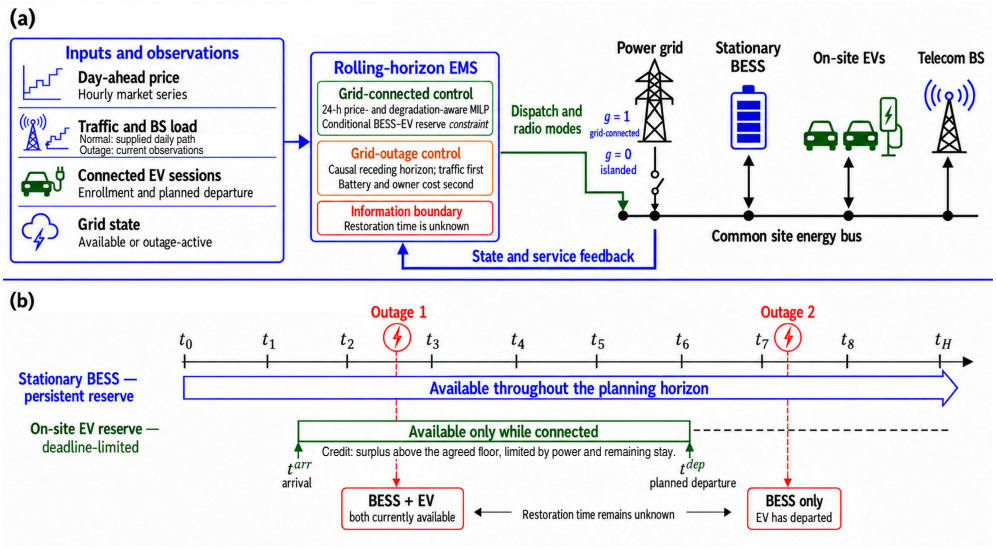


Fig. 1 Site architecture and storage availability: (a) coordinated energy management; (b) persistent and deadline-limited reserves.

$$\sum_{m\in\mathcal{M}_t} z_{t,m} = 1, \qquad z_{t,m} \in \{0,1\}. \tag{1}$$

$$\ell_t = \sum_{m\in\mathcal{M}_t} \ell_{t,m} z_{t,m}, \qquad q_t = \sum_{m\in\mathcal{M}_t} q_{t,m} z_{t,m}. \tag{2}$$

The binary variable $z_{t,m}$ indicates the selected mode. Each mode specifies a set of active carriers, requiring site power $\ell_{t,m}$ in kW and carrying traffic $q_{t,m}$ in GB/h; ℓ_t and q_t are the resulting power and traffic rate. The available modes include full service, complete shutdown, and partial service with the required coverage carriers retained. Dominated power–traffic combinations are removed, while full service is retained as a benchmark. Traffic associated with inactive carriers is unserved; traffic redistribution and user reassociation are excluded. All compared policies use the same mode set. This representation accounts for radio-dependent power consumption and service loss during outages [17, 18]. Mode construction is specified in Section 5.

$$g_t + p_t^{\mathrm{B},-} + \sum_{i\in\mathcal{I}_t} p_{i,t}^{\mathrm{E},-} = \ell_t^{\mathrm{full}} + p_t^{\mathrm{B},+} + \sum_{i\in\mathcal{I}_t} p_{i,t}^{\mathrm{E},+}. \tag{3}$$

$$p_t^{\mathrm{B},-} + \sum_{i\in\mathcal{I}_t} p_{i,t}^{\mathrm{E},-} = \ell_t + p_t^{\mathrm{B},+}. \tag{4}$$

Equation (3) applies during normal operation, when all offered traffic is served and $g_t \geq 0$ denotes telecom grid import. Equation (4) applies during outages, when grid import and EV charging are zero. The set $\mathcal{I}_t$ contains connected, enrolled EV sessions. Powers $p_t^{\mathrm{B},\pm}$ and $p_{i,t}^{\mathrm{E},\pm}$ are measured at the site bus; $+$ and $-$ denote charging and discharging of the BESS and EV session i, respectively.

Normal-operation EV powers represent telecom-controlled charging and discharging relative to an owner-charging reference. Reference charging occupies port capacity but is accounted for separately from telecom grid import. Equation (3) is therefore the incremental telecom balance. In the evaluated base scenario, reference charging is zero, so it also represents the physical site balance.

3.3 Stationary and temporary storage

Let e_t^{B} denote stationary-battery cell energy at the start of interval t. In both operating regimes, its dynamics, energy bounds, and converter constraints are

$$e_{t+1}^{\mathrm{B}} = e_t^{\mathrm{B}} + \left(\eta^{\mathrm{B},+} p_t^{\mathrm{B},+} - \frac{p_t^{\mathrm{B},-}}{\eta^{\mathrm{B},-}} \right) \Delta t. \tag{5}$$

$$\underline{e}^{\mathrm{B}} \le e_t^{\mathrm{B}} \le \overline{e}^{\mathrm{B}}. \tag{6}$$

$$0 \le p_t^{\mathrm{B},+} \le \overline{p}^{\mathrm{B},+} u_t, \qquad 0 \le p_t^{\mathrm{B},-} \le \overline{p}^{\mathrm{B},-} (1 - u_t), \qquad u_t \in \{0, 1\}. \tag{7}$$

Efficiencies $\eta^{\mathrm{B},+}$ and $\eta^{\mathrm{B},-}$ convert between bus and cell energy. For nominal capacity C^{B}, the bounds $\underline{e}^{\mathrm{B}}$ and $\overline{e}^{\mathrm{B}}$ correspond to the allowed SOC range. The barred powers are converter limits, and u_t prevents simultaneous BESS charging and discharging. Capacity remains fixed during dispatch; calendar and cycle degradation enter the costs in Section 4 [4, 13, 19].

$$R_t^{\mathrm{B}} = \eta^{\mathrm{B},-} \left(e_t^{\mathrm{B}} - \underline{e}^{\mathrm{B}} \right). \tag{8}$$

$$e_N^{\mathrm{B}} = e_0^{\mathrm{B}}. \tag{9}$$

The quantity R_t^{B} is bus energy deliverable above the physical minimum, subject to the discharge-power limit. Equation (9) applies only to the normal-operation study: it prevents reported savings from including a net withdrawal of initial stationary energy. States carry between scheduling windows without daily resets. Sampled outages start from the corresponding normal-operation states and are evaluated separately.

An enrolled EV session i has arrival boundary a_i, declared departure boundary d_i, capacity C_i, and protected departure energy e_i^{dep}. It is connected during intervals $a_i \le t < d_i$. During normal operation, its cell energy is represented by a reference trajectory $\widehat{e}_{i,t}$ without telecom dispatch and a signed deviation $\delta_{i,t}$:

$$e_{i,t}^{\mathrm{E}} = \widehat{e}_{i,t} + \delta_{i,t}. \tag{10}$$

$$\delta_{i,t+1} = \delta_{i,t} + \left(\eta_i^{\mathrm{E},+} p_{i,t}^{\mathrm{E},+} - \frac{p_{i,t}^{\mathrm{E},-}}{\eta_i^{\mathrm{E},-}} \right) \Delta t, \qquad a_i \le t < d_i. \tag{11}$$

$$-\overline{D}_i^{\mathrm{E}} C_i \le \delta_{i,t} \le 0, \qquad \underline{e}_i^{\mathrm{E}} \le e_{i,t}^{\mathrm{E}} \le \overline{e}_i^{\mathrm{E}}, \qquad a_i \le t \le d_i. \tag{12}$$

$$\delta_{i,a_i} = 0, \qquad e_{i,d_i}^{\mathrm{E}} \ge e_i^{\mathrm{dep}}. \tag{13}$$

EV efficiencies have the same bus–cell interpretation as for the BESS. The dimensionless parameter $\overline{D}_i^{\mathrm{E}}$ limits the net energy deficit relative to the reference, as a fraction of capacity; it does not limit cumulative discharge. The restriction $\delta_{i,t} \leq 0$ allows withdrawal and restoration of owner energy but excludes charging above the reference trajectory. Connection times and protected energy delimit the flexibility accessible to the site [6, 14].

In the evaluated agreement, $e_i^{\mathrm{dep}} = \underline{e}_i^{\mathrm{E}}$: the agreed floor is protected, but departure at the arrival or reference SOC is not promised. Reference charging is zero, so $\widehat{e}_{i,t}$ remains equal to arrival energy throughout the session. Energy not restored before departure is included in owner compensation in Section 4.

$$\sum_{i \in \mathcal{I}_{j,t}} \left(p_{i,t}^{\mathrm{E},+} + p_{i,t}^{\mathrm{E},-} \right) \leq \overline{p}_j - b_{j,t}^{\mathrm{ref}}, \qquad j \in \mathcal{J}. \tag{14}$$

$$\sum_{i \in \mathcal{I}_t} p_{i,t}^{\mathrm{E},+} \leq \overline{P}^{\mathrm{EV}} u_t, \qquad \sum_{i \in \mathcal{I}_t} p_{i,t}^{\mathrm{E},-} \leq \overline{P}^{\mathrm{EV}} (1 - u_t). \tag{15}$$

The set $\mathcal{J}$ contains charging ports, and $\mathcal{I}_{j,t}$ contains sessions connected to port j. Its bidirectional limit is $\overline{p}_j$, and reference charging occupies power $b_{j,t}^{\mathrm{ref}}$, where $0 \leq b_{j,t}^{\mathrm{ref}} \leq \overline{p}_j$. Total port capacity is $\overline{P}^{\mathrm{EV}} = \sum_{j \in \mathcal{J}} \overline{p}_j$. Each evaluated port serves at most one vehicle at a time. Session powers also respect their assigned converter limits, with the EV discharge limit $\overline{p}_i^{\mathrm{E},-}$ not exceeding its port capacity. EV powers are nonnegative and zero outside the connection interval.

Equation (15) applies only during normal operation. Sharing u_t with the BESS prevents simultaneous controlled charging and discharging across storage resources. During outages, EV charging is zero and EV discharge is independent of BESS direction, allowing a vehicle to supply the site while charging the stationary battery.

$$e_{i,t+1}^{\mathrm{E}} = e_{i,t}^{\mathrm{E}} - \frac{p_{i,t}^{\mathrm{E},-}}{\eta_i^{\mathrm{E},-}} \Delta t, \qquad e_{i,t+1}^{\mathrm{E}} \geq e_i^{\mathrm{dep}}, \qquad i \in \mathcal{I}_t. \tag{16}$$

Equation (16) governs connected EVs during outages. Vehicles already present retain their controlled pre-outage states; a later arrival introduces its energy only when observed. Withdrawals reduce the remaining energy budget, and departure removes the vehicle from site access.

3.4 Standby-equivalent reserve sharing

The standby reference maintains stationary energy e^{SB} during normal operation and uses the battery only during outages. Its deliverable energy defines a common reserve target for policies that allow EV-enabled stationary dispatch:

$$R^{\star} = \eta^{\mathrm{B},-} \left(e^{\mathrm{SB}} - \underline{e}^{\mathrm{B}} \right). \tag{17}$$

$$P_t^{\mathrm{svc}} = \min_{\substack{m \in \mathcal{M}_t \\ q_{t,m} \geq \rho q_t^{\mathrm{full}}}} \ell_{t,m}. \tag{18}$$

$$P^{\mathrm{des}} = Q_\xi\left(\{P_t^{\mathrm{svc}}\}_{t=0}^{N-1}\right), \qquad H^{\mathrm{SB}} = \frac{R^\star}{P^{\mathrm{des}}}. \tag{19}$$

Here P_t^{svc} is the minimum mode power required to serve a fraction $\rho \in (0,1]$ of offered traffic. The operator Q_ξ gives its empirical quantile at level $\xi \in (0,1)$, yielding design power $P^{\mathrm{des}} > 0$. The duration H^{SB} is an energy-to-power reference used to cap EV reserve credit, not a guaranteed backup duration. The target $R^\star$ remains fixed, and vehicles need not remain connected for the entire reference duration.

Let $\mathcal{I}_t^{\mathrm{R}} \subseteq \mathcal{I}_t$ contain connected sessions whose reference energy exceeds their protected floor. Their credited cell energy $c_{i,t}$ satisfies

$$0 \le c_{i,t} \le e_{i,t}^{\mathrm{E}} - e_i^{\mathrm{dep}}, \qquad i \in \mathcal{I}_t^{\mathrm{R}}. \tag{20}$$

$$c_{i,t} \le \frac{\overline{p}_i^{\mathrm{E},-}}{\eta_i^{\mathrm{E},-}} \min\left\{H^{\mathrm{SB}}, (d_i - t)\Delta t\right\}, \qquad i \in \mathcal{I}_t^{\mathrm{R}}. \tag{21}$$

$$c_{i,t} = 0 \quad \text{for } i \notin \mathcal{I}_t^{\mathrm{R}}, \qquad R_t^{\mathrm{EV}} = \alpha \sum_{i \in \mathcal{I}_t^{\mathrm{R}}} \eta_i^{\mathrm{E},-} c_{i,t}. \tag{22}$$

Credit is limited by actual energy above the protected floor, discharge power, and remaining connection time. The factor $\alpha \in [0,1]$ discounts credited bus energy; it is a scenario parameter, not an estimated reliability or participation probability. Only connected vehicles receive credit, which expires at departure. Scheduled future arrivals therefore cannot support current reserve.

$$R_t^{\mathrm{B}} + R_t^{\mathrm{EV}} \ge R^\star, \qquad t = 0, \dots, N. \tag{23}$$

$$R_{t+1}^{\mathrm{B}} + R_t^{\mathrm{EV}} \ge R^\star, \qquad t = 0, \dots, N-1. \tag{24}$$

$$e_t^{\mathrm{B}} \ge \underline{e}^{\mathrm{B}} + \frac{[R^\star - R_t^{\mathrm{EV}}]^+}{\eta^{\mathrm{B},-}}, \qquad [x]^+ = \max\{x, 0\}. \tag{25}$$

Equation (23) enforces the target at every normal-operation boundary, including scheduling-window endpoints. Equation (24) constrains the next BESS state using current EV credit, preventing discharge that relies on a vehicle arriving at the next boundary. Together with the physical BESS lower bound, Eq. (25) restates Eq. (23): connected EV reserve reduces the stationary energy that must be retained, without requiring routine EV discharge. Without EV credit, the BESS must retain at least e^{SB}; as credit expires, the corresponding stationary reserve must be restored.

These constraints apply during normal operation. During outages, dispatch uses the remaining physical energy and power limits. Equal credited energy does not ensure equal backup duration, because EV access can end and future loads vary. The outage evaluation therefore assesses the service consequences of reserve sharing rather than assuming unchanged reliability.

3.5 Information available to the controllers

During normal operation, the planner receives day-ahead prices, the supplied demand path, and scheduled EV sessions within its planning window. The evaluated scenario provides realized load, so normal-operation results are conditional on perfect demand information rather than a validated forecasting method.

During an outage, the controller observes current storage states, radio demand, connected vehicles, and their declared departures. It has no access to future arrivals, future traffic measurements, or the actual grid-restoration time. Radio forecasts and outage survival weights are defined as

$$\widehat{\ell}_{t+k,m|t} = \ell_{t,m}, \qquad \widehat{q}_{t+k,m|t} = q_{t,m}, \qquad k = 0, \dots, K-1. \tag{26}$$

$$w_{t,k} = \Pr\{T^{\text{out}} > (r_t + k)\Delta t \,|\, T^{\text{out}} > r_t \Delta t\} = \exp\left(-\frac{k\Delta t}{\tau}\right). \tag{27}$$

Equation (26) holds the current mode-specific power and traffic observations over a fixed horizon of K intervals; k is the forecast offset and $m \in \mathcal{M}_t$. In Eq. (27), T^{out} denotes total outage duration, r_t is elapsed outage time in intervals, and $\tau > 0$ is the mean of an assumed exponential restoration prior. Thus, $w_{t,k}$ is the conditional probability that the outage persists to the start of forecast interval k. Its independence from elapsed time follows from the memoryless prior, which is a scenario assumption rather than a fit to the evaluated outages.

The controller replans using updated observations, and an arriving EV enters the plan only after connection. The horizon is not shortened using the realized restoration time. Dispatch objectives and the update procedure are specified in Section 4.

EV arrival energy, enrollment, and protected energy are scenario inputs, not quantities inferred from charging records. Declared departures are respected in the base scenario. Data provenance and numerical settings are reported in Section 5.

4 Optimization and Control Framework

EV reserve makes stationary energy available for use; it does not determine whether using that energy is worthwhile. The controller therefore accounts for electricity purchases, battery wear and owner compensation. With grid supply available, it minimizes scheduling cost while serving all offered traffic and retaining the standby-equivalent reserve defined in Section 3. During an outage, carried traffic takes priority, and cost determines how that service is supplied.

4.1 Battery wear in scheduling and assessment

Cycle wear is represented in dispatch by a depth-dependent piecewise-affine (PWA) surrogate. Incorporating marginal cycle-aging costs into market scheduling is an established approach [13]; the ordered-depth implementation below is the surrogate used in this study. Let x identify the BESS or an EV session, with capacity C_x and replacement cost c_x^{rep} per cell-kWh. Define

Table 2 Main notation.

Symbol	Definition	Symbol	Definition
t	Time index	$\mathcal{I}_t$	Connected, enrolled EV sessions
N	Study length [intervals]	a_i, d_i	Arrival/departure indices
Δt	Interval duration [h]	$\widehat{e}_{i,t}$	Reference EV energy [kWh]
$\mathcal{M}_t$	Feasible radio modes	$\delta_{i,t}$	EV energy deviation [kWh]
$z_{t,m}$	Mode-selection binary	e_i^{dep}	Protected energy [kWh]
$\ell_{t,m}$	Mode power [kW]	$\overline{D}_i^{\mathrm{E}}$	Maximum net withdrawal fraction
$q_{t,m}$	Mode traffic [GB/h]	$\mathcal{J}$	Charging ports
g_t	Telecom grid import [kW]	$\overline{p}_j$	Port power limit [kW]
e_t^{B}	BESS cell energy [kWh]	$b_{j,t}^{\mathrm{ref}}$	Reference charging [kW]
$e_{i,t}^{\mathrm{E}}$	EV cell energy [kWh]	e^{SB}	Standby cell energy [kWh]
C^{B}, C_i	Nominal capacities [kWh]	$R^\star$	Bus-energy reserve target [kWh]
$\underline{e}^x, \overline{e}^x$	Cell-energy bounds [kWh]	$R_t^{\mathrm{B}}, R_t^{\mathrm{EV}}$	Bus-energy reserves [kWh]
$p^{x,+}, p^{x,-}$	Bus charging/discharging [kW]	$c_{i,t}$	Credited EV cell energy [kWh]
$\overline{p}^{x,+}, \overline{p}^{x,-}$	Storage power limits [kW]	α	EV credit discount
$\eta^{x,+}, \eta^{x,-}$	One-way efficiencies	ρ	Reference traffic fraction
u_t	Direction binary	ξ	Design-quantile level
K	Horizon [intervals]	P^{des}	Design power [kW]
r_t	Elapsed outage [intervals]	H^{SB}	Reference standby duration [h]
T^{out}	Outage duration [h]	τ	Restoration-prior mean [h]
$w_{t,k}$	Conditional survival weight	$\widehat{\ell}, \widehat{q}$	Power/traffic forecasts

$x \in \{\mathrm{B}, \mathrm{E}\}$ denotes stationary or EV storage; EV quantities also carry index i. Superscripts $+$ and $-$ denote charging and discharging; full denotes full service.

$$\Phi_x(D) = \frac{1}{N_{80,x}(D)}, \qquad D > 0, \qquad \Phi_x(0) = 0. \tag{28}$$

$$\beta_{x,r} = \frac{\Phi_x(D_{x,r}) - \Phi_x(D_{x,r-1})}{D_{x,r} - D_{x,r-1}}, \qquad r = 1, \ldots, J_x. \tag{29}$$

$$d_{\mathrm{B},t} = \frac{\overline{e}^{\mathrm{B}} - e_t^{\mathrm{B}}}{C^{\mathrm{B}}}, \qquad d_{i,t} = -\frac{\delta_{i,t}}{C_i}. \tag{30}$$

Here $N_{80,x}(D)$ is the specified cycle life at depth D to an 80% remaining-capacity threshold. Thus, Φ_x represents consumption of a modeled life-loss budget, rather than capacity fade itself. The increasing nodes $D_{x,0} = 0, \ldots, D_{x,J_x}$ and nonnegative slopes $\beta_{x,r}$ come from the chemistry-specific input curves. Active BESS depth is measured below its upper energy bound; EV depth measures borrowing below its reference trajectory. In outage planning, the observed EV depth is carried forward and increases by additional withdrawn cell energy divided by C_i.

$$y_{x,t,r} = \min\Big\{ D_{x,r} - D_{x,r-1}, \, [d_{x,t} - D_{x,r-1}]^+ \Big\}. \tag{31}$$

$$\sum_{n=0}^{J_x} \omega_{x,t,n} = 1, \qquad d_{x,t} = \sum_{n=0}^{J_x} D_{x,n}\omega_{x,t,n},$$
$$\omega_{x,t,n} \geq 0, \qquad \{\omega_{x,t,n}\}_{n=0}^{J_x} \text{ is SOS2}, \tag{32}$$
$$y_{x,t,r} = \sum_{n=0}^{J_x} \omega_{x,t,n} \min\left\{D_{x,r} - D_{x,r-1}, [D_{x,n} - D_{x,r-1}]^+\right\}.$$

$$h_{x,t,r} \geq y_{x,t+1,r} - y_{x,t,r}, \qquad 0 \leq h_{x,t,r} \leq D_{x,r} - D_{x,r-1}. \tag{33}$$

$$K_x^{\text{cyc,plan}}(\mathcal{W}) = \kappa C_x c_x^{\text{rep}} \sum_{t\in\mathcal{W}_x} \sum_{r=1}^{J_x} \beta_{x,r} h_{x,t,r}. \tag{34}$$

The fill $y_{x,t,r}$ is the occupied part of segment r. In Eq. (32), a special ordered set of type 2 (SOS2) permits at most two adjacent interpolation weights to be nonzero. Interpolating each segment's fill at those same nodes gives Eq. (31) exactly; an equivalent ordered-binary formulation is used when SOS2 is unavailable. The nonnegative increment $h_{x,t,r}$ charges for deeper withdrawal without giving a negative wear credit for recharge. Set $\mathcal{W}_x$ contains the connected intervals of battery x within window $\mathcal{W}$, and κ is a declared pack-level damage multiplier. These constraints are linear after the segment encoding; they do not implement rainflow counting inside the optimizer.

Calendar exposure is included separately because degradation during storage depends on SOC and temperature [4]. The BESS scheduling term is

$$K_{\text{B}}^{\text{cal,plan}}(\mathcal{W}) = \kappa C^{\text{B}} c_{\text{B}}^{\text{rep}} \sum_{t\in\mathcal{W}} \widehat{\psi}_{\text{B}}\left(\frac{e_t^{\text{B}}}{C^{\text{B}}}, \theta_{\text{B}}\right) \Delta t. \tag{35}$$

Function $\widehat{\psi}_{\text{B}}$ is the PWA life-loss rate per hour at the declared temperature θ_{B}, obtained from the input SOC nodes with adjacent-node interpolation. This rate is a scheduling approximation. Reported wear is recomputed from the realized trajectories:

$$L_x^{\text{cyc,RF}} = \kappa \sum_{c\in\mathcal{R}_x} n_c \Phi_x(D_c). \tag{36}$$

$$U_{x,t+1} = A_{x,t}\left[\left(\frac{U_{x,t}}{A_{x,t}}\right)^{1/p_{x,t}} + \frac{\Delta t}{T_{x,t}^{\text{ref}}}\right]^{p_{x,t}}, \qquad U_{x,t_0} = 0. \tag{37}$$

$$\begin{aligned} K_{\text{B}}^{\text{wear,ass}} &= C^{\text{B}} c_{\text{B}}^{\text{rep}}\left(L_{\text{B}}^{\text{cyc,RF}} + L_{\text{B}}^{\text{cal}}\right), \\ K_i^{\text{wear,ass}} &= C_i c_i^{\text{rep}}\left(L_i^{\text{cyc,RF}} + \left[L_i^{\text{cal,ctrl}} - L_i^{\text{cal,ref}}\right]^+\right). \end{aligned} \tag{38}$$

Set $\mathcal{R}_x$ contains rainflow-counted cycles with depth D_c and count n_c: one for a full cycle and one-half for a residual half-cycle. The BESS trace retains cycles across daily boundaries; EV cycle attribution uses the incremental borrowing trace $1 + \delta_{i,t}/C_i$. For calendar assessment, $A_{x,t} > 0$, $p_{x,t} > 0$ and $T_{x,t}^{\text{ref}} > 0$ are the reference loss, time exponent and reference duration in hours, interpolated at interval-average SOC and temperature. State $U_{x,t}$ advances through an equivalent-age mapping, with

$L_x^{\mathrm{cal}} = \kappa U_{x,b}$ at the final boundary b; t_0 is the start of the assessed trace. For EVs, controlled and reference calendar losses are evaluated over the same session. This is an attribution model for incremental wear, not a validated prediction of individual vehicle life. Surrogate and assessed costs are retained separately, since their difference can affect reported savings.

4.2 Energy reimbursement and owner margin

Owner compensation covers unreplaced energy and attributed wear, with a separate participation margin. This distinction follows degradation-aware economic assessments of EV use [6, 7]; the coefficients below specify the agreement assumed in this study. For a normal window $\mathcal{W}_s = \{s, \dots, b_s - 1\}$, let $\mathcal{I}(\mathcal{W}_s)$ contain its overlapping sessions and $\mathcal{W}_{s,i}$ the connected intervals of session i. Define

$$V_i^{\mathrm{use}}(\mathcal{W}_s) = \frac{c^{\mathrm{ret}}}{\eta_i^{\mathrm{E},+}\eta_i^{\mathrm{E},-}} \sum_{t \in \mathcal{W}_{s,i}} p_{i,t}^{\mathrm{E},-} \Delta t. \tag{39}$$

$$\begin{aligned} \Pi_i^{\mathrm{nor,plan}}(\mathcal{W}_s) = \mu \left[V_i^{\mathrm{use}}(\mathcal{W}_s) + K_i^{\mathrm{cyc,plan}}(\mathcal{W}_s) \right] \\ + \sigma \sum_{t \in \mathcal{W}_{s,i}} \left[\lambda_t - c^{\mathrm{ret}} \right]^+ p_{i,t}^{\mathrm{E},-} \Delta t. \end{aligned} \tag{40}$$

$$\begin{aligned} C_{\mathrm{E}}^{\mathrm{own,nor,plan}}(\mathcal{W}_s) = \sum_{i \in \mathcal{I}(\mathcal{W}_s)} \frac{c^{\mathrm{ret}}}{\eta_i^{\mathrm{E},+}} \left[-\delta_{i,b_{s,i}} \right]^+ \\ + \sum_{i \in \mathcal{I}(\mathcal{W}_s)} \left[K_i^{\mathrm{cyc,plan}}(\mathcal{W}_s) + \Pi_i^{\mathrm{nor,plan}}(\mathcal{W}_s) \right]. \end{aligned} \tag{41}$$

Price λ_t is the site's electricity price, and c^{ret} is the declared owner replenishment tariff, both in €/kWh. V_i^{use} values contributed energy including conversion losses; it is not an additional reimbursement of energy already returned in kind. The markup $\mu \geq 0$ applies to that value and wear, while $\sigma \in [0, 1]$ allocates a share of positive spot-price surplus to the owner. Grid purchases already include energy used for EV recharge. The first term of Eq. (41) therefore values only the outstanding cell-energy deficit. For a session continuing beyond b_s, it is a terminal liability used in planning, not another cash payment at every window boundary. Reported compensation settles the session's remaining deficit once and replaces planned wear by $K_i^{\mathrm{wear,ass}}$. Owner profit comprises the margin and spot bonus; energy and wear reimbursements are excluded from it. Availability fees and minimum-profit guarantees are zero in the base agreement, and enrollment is assumed rather than inferred from owner acceptance.

4.3 Normal-operation optimization

For each policy permitting economic dispatch, the normal planner solves

$$\min_{\boldsymbol{x}\in\mathcal{F}^{\mathrm{nor}}_{s,\mathrm{pol}}} \quad \sum_{t\in\mathcal{W}_s} \lambda_t g_t \Delta t + K^{\mathrm{cyc,plan}}_{\mathrm{B}}(\mathcal{W}_s) + K^{\mathrm{cal,plan}}_{\mathrm{B}}(\mathcal{W}_s) + C^{\mathrm{own,nor,plan}}_{\mathrm{E}}(\mathcal{W}_s) + \varepsilon_{\mathrm{th}} \sum_{t\in\mathcal{W}_s} p^{\mathrm{B},-}_t \Delta t - \nu_s e^{\mathrm{B}}_{b_s}. \tag{42}$$

$$\nu_s = \eta^{\mathrm{B},-} \max\{0, \mathrm{median}_{t\in\mathcal{W}_s}\, \lambda_t\}\,. \tag{43}$$

The vector $\boldsymbol{x}$ includes energy states, storage powers, grid import and the direction and PWA variables. $\mathcal{F}^{\mathrm{nor}}_{s,\mathrm{pol}}$ comprises the physical, EV-floor and reserve constraints in Section 3, together with the policy restrictions below. The small coefficient $\varepsilon_{\mathrm{th}}$ [€/kWh] resolves ties in BESS throughput; ν_s [€/cell-kWh] assigns a terminal value to stationary inventory. Neither term is reported as realized income. The planner uses daily windows with carried storage states and the study-period inventory closure in Eq. (9). Normal EV calendar differences enter reported compensation but not this dispatch objective. Consequently, minimizing the scheduling surrogate does not guarantee the lowest assessed annual cost.

No BESS-first or EV-first discharge order is imposed. Dispatch depends on prices, conversion losses, active wear segments, compensation and reserve feasibility. A large price spread need not justify EV withdrawal once its full contribution cost is included.

4.4 Causal outage control

At an outage update t, the controller plans over $\mathcal{W}^{\mathrm{out}}_t = \{t, \ldots, t+K-1\}$ using the current-observation forecasts and survival weights defined in Eqs. (26) and (27). Its two objectives are solved in sequence:

$$Q_t(\boldsymbol{x}) = \sum_{k=0}^{K-1} w_{t,k} \sum_{m\in\mathcal{M}_t} \widehat{q}_{t+k,m|t} z_{t+k,m} \Delta t. \tag{44}$$

$$\max_{\boldsymbol{x}\in\mathcal{F}^{\mathrm{out}}_{t,\mathrm{pol}}} Q_t(\boldsymbol{x}). \tag{45}$$

$$\begin{aligned} \min_{\boldsymbol{x}\in\mathcal{F}^{\mathrm{out}}_{t,\mathrm{pol}}} \quad & K^{\mathrm{cyc,plan}}_{\mathrm{B}}(\mathcal{W}^{\mathrm{out}}_t) + C^{\mathrm{own,out,plan}}_{\mathrm{E}}(\mathcal{W}^{\mathrm{out}}_t) \\ \text{subject to} \quad & Q_t(\boldsymbol{x}) \geq \widetilde{Q}_t - \varepsilon_Q. \end{aligned} \tag{46}$$

$$\begin{aligned} C^{\mathrm{own,out,plan}}_{\mathrm{E}}(\mathcal{W}^{\mathrm{out}}_t) = (1+\mu) \sum_{i\in\mathcal{I}_t} \left[V^{\mathrm{use}}_i(\mathcal{W}^{\mathrm{out}}_t) + K^{\mathrm{cyc,plan}}_i(\mathcal{W}^{\mathrm{out}}_t) \right] \\ + \pi^{\mathrm{out}} \sum_{i\in\mathcal{I}_t} \sum_{u\in\mathcal{W}^{\mathrm{out}}_{t,i}} p^{\mathrm{E},-}_{i,u} \Delta t. \end{aligned} \tag{47}$$

The forecast uses the presently observed mode set $\mathcal{M}_t$. The feasible set $\mathcal{F}^{\mathrm{out}}_{t,\mathrm{pol}}$ enforces outage power balance, physical storage limits, observed EV energy, announced departures and admissible radio modes. The first stage supplies a feasible service incumbent $\widetilde{Q}_t$ with a recorded optimization gap. The second preserves that incumbent within tolerance ε_Q [GB] and minimizes its supply cost; it does not claim an exact first-stage optimum when a gap remains. The energy-value definition in Eq. (39) also applies

to the outage window. Here $\mathcal{W}^{\text{out}}_{t,i}$ contains the planning-horizon intervals before EV i's announced departure, and π^{out} [€/bus-kWh] is an optional emergency premium, zero in the base agreement. All withdrawn EV energy is reimbursed because it cannot be restored by grid charging during the event. The normal spot bonus is absent. Survival weights apply to service; the secondary cost objective values the whole planned path without survival discounting.

The normal reserve-sharing constraints are not enforced during an outage; the physical lower energy bounds remain in force. EV-to-BESS transfer is permitted by Eq. (4), subject to conversion losses, owner payments and cycling costs. It can retain energy at the site after an EV departs, but need not be selected if direct supply serves the objective better. Only the actions up to the next scheduled or observation-triggered update are implemented. The evaluated controller replans hourly and on new radio or EV observations, with an eight-hour horizon that does not depend on the realized restoration time. Calendar aging and post-restoration recovery are excluded from the outage scheduling objective.

All dispatch problems are mixed-integer linear programs (MILPs), including the direction and PWA constraints. The service stage omits the cost-only aging auxiliaries; the cost stage adds them while preserving service. Feasible incumbents and objective bounds are retained, and each solve must meet a declared relative or absolute gap. Solver settings are reported in Section 5.

4.5 Policies and comparisons

Four policies use the same BESS hardware, prices, offered traffic, underlying EV-session scenario and carrier-aware outage modes. They differ in whether EV energy and reserve credit are accessible to the controller:

- **Standby.** Grid supply serves normal demand and the BESS is held at e^{SB}. It is used only during outages; EV energy is excluded from both dispatch and reserve credit.
- **EV Backup.** Normal operation is identical to Standby. Connected EVs can supply energy during outages, with the stated compensation. Their presence does not release stationary reserve for normal dispatch.
- **EV Reserve.** Connected EV credit permits economic BESS dispatch under Eqs. (23) and (24). Controlled EV charging and discharging are zero during normal operation. EVs can support outages.
- **Joint Dispatch.** The same reserve-sharing rule and outage actions as EV Reserve apply, while economic EV withdrawal and restoration are also permitted during normal operation under Eq. (42).

Standby versus EV Backup examines outage activation without changing the normal schedule. EV Backup versus EV Reserve examines the reserve-sharing strategy; EV Reserve versus Joint Dispatch examines additional routine EV dispatch. Comparisons start outages from each policy's own normal-operation states, so reserve release can affect subsequent service as well as cost. A separate matched-state comparison starts with EV Reserve's stationary energy and compares outage support with and without EVs. It isolates recourse at that initial state; the EV-disabled arm is not a compliant stationary-only normal schedule. A one-step outage benchmark uses Joint

Dispatch's initial storage states, admissible radio modes and observation rules, with $K = 1$, to examine the effect of look-ahead. No realized future information is supplied to either controller.

4.6 Operating cost and deployment value

Reported normal-operation cost uses realized purchases, assessed BESS wear and settled owner payments, excluding scheduling tie-breaks and salvage rewards. For an independently evaluated outage event j of duration D, its incremental cost is estimated as

$$\begin{aligned}\widetilde{C}^{\mathrm{out}}_{j,\mathrm{pol}}(D) = C^{\mathrm{act}}_{j,\mathrm{pol}}(D) - C^{\mathrm{grid,nor}}_{j,\mathrm{pol}}(D) - C^{\mathrm{own,nor,var}}_{j,\mathrm{pol}}(D) \\ - K^{\mathrm{cyc,nor,local}}_{j,\mathrm{pol}}(D) + \frac{\lambda^{+}_{j,\mathrm{rest}}}{\eta^{\mathrm{B},+}}\left(e^{\mathrm{B,nor}}_{j,\mathrm{end}} - e^{\mathrm{B,out}}_{j,\mathrm{end}}\right).\end{aligned} \tag{48}$$

Here C^{act} includes assessed outage cycle wear and EV payments. The three subtracted terms are displaced normal grid expenditure, allocated variable owner payments and local BESS cycle wear over the same interval. The last term settles the difference in ending BESS inventory at the nonnegative restoration-time price $\lambda^{+}_{j,\mathrm{rest}}$. An energy surplus receives a credit rather than being discarded. This settlement uses information available for ex-post assessment, not for control. It approximates recovery expenditure without simulating its power limits, calendar-loss difference or effects on later dispatch; local cycle wear and allocated owner payments are also event-accounting approximations.

$$\begin{aligned}\mathcal{V}_{\mathrm{pol|ref}}(f, v; D) = S^{\mathrm{nor}}_{\mathrm{pol|ref}} - f\,\overline{\Delta\widetilde{C}}^{\mathrm{out}}(D) \\ + fv\,\overline{\Delta Q}^{\mathrm{out}}(D) - \Delta C^{\mathrm{ann}}_{\mathrm{EVSE}}.\end{aligned} \tag{49}$$

$$\Pi^{\mathrm{ann}}_{\mathrm{EV,pol}}(f; D) = \Pi^{\mathrm{nor}}_{\mathrm{EV,pol}} + f\,\overline{\left(\Pi^{\mathrm{out}}_{\mathrm{EV,pol}}(D) - \Pi^{\mathrm{nor,disp}}_{\mathrm{EV,pol}}(D)\right)}. \tag{50}$$

In Eq. (49), $S^{\mathrm{nor}}_{\mathrm{pol|ref}}$ is the reference's annual normal cost minus the candidate's. The barred quantities are weighted common-start mean differences, candidate minus reference, in incremental cost [€/event] and realized carried traffic [GB/event]. This traffic is unweighted by the controller's survival prior. Frequency f is events/year, and v is an assumed service value in €/GB, not a measured loss tariff. The infrastructure difference $\Delta C^{\mathrm{ann}}_{\mathrm{EVSE}}$ includes annualized additional charger and integration costs and maintenance; it cancels when both alternatives require the same installation. The main comparisons assume existing compatible infrastructure and set this incremental cost to zero; a nonzero term represents additional installation in the separate deployment screen. Equation (50) similarly adds outage owner profit to normal annual profit while removing displaced normal variable profit. Reimbursements are excluded from these profit terms.

The frequency sweep reweights the sampled events without rerunning annual dispatch. Both service and cost differences retain their signs, so more outages need not improve value. The calculation is conditional on duration D and the sampled-start distribution; it is not a chronological simulation of repeated outages, recovery or heatwave clustering. It also does not adjust normal scheduling or owner agreements as

frequency changes. Section 5 specifies the sampling weights, infrastructure scenarios and screening limits.

5 Evaluation Methodology and Simulation Setup

The four policies in Section 4.5 use common equipment and radio controls. Annual dispatch establishes each policy's storage states; paired outages then assess the service and cost consequences of those states. Owner profit and infrastructure cost are reported separately from operating savings.

5.1 Input data and fleet scenario

The radio input comprises 32 complete days of hourly records from one BS, from 12 December 2023 to 12 January 2024. Three sectors contain LTE 800, LTE 1800, LTE 2100 and NR 3700 carriers, with some missing carrier records. Uplink and downlink volumes are added, following the CSV's declared byte units, and divided by 10^9 to obtain GB per recorded hour. No traffic multiplier is applied. The original operator counter definitions and aggregation basis were not independently verified; absolute traffic volumes and valuations are therefore conditional on the declared units.

Carrier power estimates are scaled at each source hour to reconcile their sum with recorded radio power. A declared 0.26 kW shared-site load is added to every active mode. Carrier subsets retain the three observed LTE 800 coverage anchors; absent carriers are excluded, and dominated power–traffic combinations are removed. Full service is retained as a benchmark, and shutdown has zero power and traffic. Traffic on inactive carriers is unserved, without reassociation. This construction is shared by all policies, so the comparisons do not attribute a different radio action set to EV participation.

Whole source days are sampled with replacement, matching weekdays and weekends, to construct the 2024 load scenario. Hourly levels are held constant over 15-min intervals. Sampling preserves within-day traffic and power relationships, but the winter trace cannot establish annual seasonal demand. The Italian and Dutch 2024 day-ahead price inputs, attributed to the ENTSO-E Transparency Platform [9], each contain 8,784 delivery hours. Prices are joined by UTC hour and converted from €/MWh to €/kWh; negative values are retained. Both markets use the same load and fleet realization. This is a comparison of wholesale price signals at a common modeled site, rather than two measured national deployments. Network charges, taxes and demand charges are excluded.

Figure 2(a) compares the distributions of hourly electricity prices and daily maximum–minimum price spreads in Italy and the Netherlands during 2024. Boxes indicate interquartile ranges, whiskers the 5th–95th percentiles, horizontal lines the medians, and diamonds the means. Panel (b) shows the source trace's median hourly aggregate traffic and site power, with shaded interquartile bands. Each series in panel (b) is normalized by its own trace mean, so the panel compares daily patterns rather than equating traffic and power units.

EV availability follows a parametric fleet scenario motivated by our conference study [8]. Four enrolled vehicles, each with a dedicated port, attend daily. Arrival

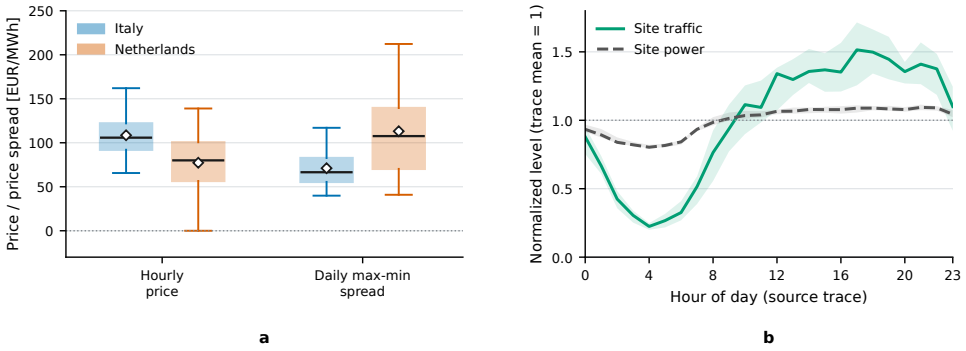


Fig. 2 Input-data characterization: (a) electricity prices and daily price spreads in Italy and the Netherlands; (b) normalized hourly site traffic and power.

time is drawn from a normal distribution with mean 08:00 and standard deviation 2 h, truncated to the day. Connection duration is drawn from a lognormal distribution whose untruncated mean and standard deviation are 7 h and 2 h, respectively, and is restricted to 1–16 h. Arrival SOC is drawn from a Beta$(2, 2)$ distribution conditional on lying between 0.40 and 0.80. These are scenario parameters, not fitted population estimates. The Utrecht office-parking dataset [10] provides a relevant workplace context, but its sessions are not replayed or directly fitted by this generator. The modeled fleet's co-location with the BS is assumed.

Sessions cannot overlap for the same vehicle. Arrivals are rounded upward and departures downward to the dispatch grid, so discretization does not add connection time. Announced and actual departures coincide in the base scenario. Reference charging is zero: the assessment concerns energy already present at arrival, with controlled withdrawals accounted for through replenishment and wear compensation. The 0.80 reference upper SOC is not a promised departure charge; the agreed floor is 0.40.

5.2 Storage, reserve and compensation settings

Table 3 summarizes the main settings. The stationary battery uses lithium iron phosphate (LFP), and EV batteries use lithium nickel manganese cobalt oxide (NMC). Hardware, owner-contract and pack-aging values are declared simulation inputs unless identified as recorded data. The BESS is common to every policy, so its acquisition cost cancels in incremental comparisons; operational wear remains in the cost account.

Power limits apply separately to charging and discharging. Efficiencies are stated in charge, then discharge order. The borrowing cap is an additional limit and does not override the EV energy floor. Common reserve equals the bus-deliverable energy between the BESS standby and minimum SOC: $0.95(0.95 - 0.10) \times 10 = 8.075$ kWh. The 95th-percentile power needed to retain 90% of offered traffic provides a common reference for describing standby autonomy and limiting EV credit. It does not impose a fixed two-hour reserve or guarantee equal outage service. Connected EV credit is limited by surplus energy, port power and remaining stay, without a minimum-stay

Table 3 Principal storage and operating settings.

Parameter	Setting	Parameter	Setting
BESS chemistry/capacity	LFP / 10 kWh	EV chemistry/capacity	NMC / 40 kWh each
BESS power limits	5 kW each	EV fleet/ports	4 / 4
BESS SOC range	0.10–0.95	EV power limits	3.7 kW/port each
BESS initial/standby SOC	0.95	EV physical SOC range	0.40–0.90
BESS efficiencies	0.95 / 0.95	EV efficiencies	0.94 / 0.94
Common bus reserve	8.075 kWh	EV agreed floor	0.40 SOC
Protected-traffic reference	0.90	EV reserve-credit factor	1.0
Design-load quantile	0.95	Normal EV borrowing cap	0.50 of capacity
Replacement cost, both	150 €/kWh	Owner energy value	0.247 €/kWh
Owner utilization markup	0.20	Positive spot-surplus share	0.50
Battery temperature	25°C	Pack-loss multiplier	1.25
End-of-life capacity	0.80 of nominal	Calendar reference fade	2% in first year
Normal horizon/update	24 h / 24 h	Outage horizon/update	8 h / 1 h

qualification. Credit factor one is a contractual scenario, not a measured probability of dependable availability.

The supplied cycle-stress tables are attributed to chemistry-specific models in [13, 19]; they are adopted as simulation curves rather than measured lifetime data for the modeled packs. Zero depth has zero damage, the tabulated stress is reconstructed as $1/N_{80}$, and the terminal segment is extended to depth one where needed. The calendar table identifies BLAST-Lite 1.1.1 as its source [20]. Its relative SOC–temperature dependence and time exponents are retained, while each chemistry is rescaled to the declared 2% first-year pack-capacity fade at 50% SOC and 25°C. This scale is an assumption, not a validated pack-aging rate. Scheduling and assessed wear follow Section 4.1; nominal capacity is held fixed during the year. Availability fees, minimum-profit guarantees and additional outage premiums are zero. Consequently, modeled owner profit does not establish willingness to enroll.

5.3 Paired annual and outage design

The reported study covers all 366 days of 2024, using one common scenario seed, 20260808, for both markets. Daily normal-operation windows carry storage states across days; equal initial and terminal BESS inventory is enforced over the annual study. Standby and EV Backup share their deterministic normal schedule; EV Reserve and Joint Dispatch each require 366 daily optimization problems per market. Normal planning uses supplied daily load, cleared prices and scheduled connections. Perfect demand information is assumed for normal planning; the outage controller receives only observations available at each update.

Twenty-four outage starts were evaluated per market. Eligible starts leave enough input data for a 24-h trajectory and the fixed eight-hour planning horizon at its last update. Sampling crosses calendar quarter with three EV conditions: usable energy at onset; no usable energy at onset but a usable arrival within 24 h; or no usable EV energy in that interval. Classification uses EV Backup's uncontrolled EV states, independently of optimized reserve release. Each nonempty stratum receives at least two

starts when its population permits, with the remaining budget allocated proportionally. Starts are sampled without replacement within strata. Eight strata are nonempty in the realized scenario. For event j, the population weight is

$$w_j = \frac{N_{h(j)}}{N_{\text{valid}}\, n_{h(j)}}. \tag{51}$$

Here $h(j)$ identifies the quarter–EV stratum, $N_{h(j)}$ counts its eligible intervals, $n_{h(j)}$ is its sampled count, and N_{valid} is the total eligible population. Thus $\sum_j w_j = 1$. The weights represent a uniform eligible-start population, not an observed distribution of grid failures. Future connections help classify evaluation cases but are hidden from online outage control.

All four policies face the same starts and realized outage inputs, beginning from their own normal-operation states. One causal 24-h path supplies exact 1-, 2-, 4-, 8-, 16- and 24-h prefixes. Neither restoration time nor the reporting endpoint is revealed to the controller. The Italian case also compares outage support with and without EVs from EV Reserve's common initial BESS state. Both markets compare Joint Dispatch with a one-step controller using the same initial resources and observation rules. These diagnostics follow Section 4.5; carrier control is common throughout, and no clairvoyant benchmark is included. The completed design contains 288 policy paths and 1,728 duration-prefix observations. Prefixes of one path are dependent and do not add independent replications.

5.4 Service and economic metrics

For policy pol and duration D, let $\mathcal{T}_{j,D}$ denote the intervals of event j, and let q_t^{pol} and ℓ_t^{pol} be its realized carried traffic rate and radio-mode site power. We report

$$Q_{j,D}^{\text{pol}} = \sum_{t\in\mathcal{T}_{j,D}} q_t^{\text{pol}}\Delta t, \qquad R_{j,D}^{\text{pol}} = \frac{Q_{j,D}^{\text{pol}}}{\sum_{t\in\mathcal{T}_{j,D}} q_t^{\text{full}}\Delta t}. \tag{52}$$

$$E_{j,D}^{\text{gap,pol}} = \max\left\{0, \sum_{t\in\mathcal{T}_{j,D}} \left(\ell_t^{\text{full}} - \ell_t^{\text{pol}}\right)\Delta t\right\}. \tag{53}$$

$$\overline{Y}_D^{\text{pol}} = \sum_j w_j Y_{j,D}^{\text{pol}}, \qquad F_D^{\text{pol}}(y) = \sum_j w_j \mathbf{1}\left\{R_{j,D}^{\text{pol}} \le y\right\}. \tag{54}$$

$$R_D^{\text{tail,pol}} = \frac{1}{\beta}\int_0^{\beta} \left(F_D^{\text{pol}}\right)^{-1}(u)\,\mathrm{d}u, \qquad \beta = 0.10. \tag{55}$$

Carried volume Q is in GB and retention R is dimensionless, with retention defined for events having positive offered volume. E^{gap} [kWh] describes the power reduction relative to full radio service, including carrier shutdown; it excludes storage charging and is not a separate measure of lost traffic. In Eq. (54), Y denotes an event metric and $\mathbf{1}\{\cdot\}$ its stated-condition indicator. F_D is the weighted empirical distribution of retention, and F_D^{-1} its generalized quantile function. Equation (55) averages the lowest 10% of its probability mass, splitting a boundary observation's weight where necessary. The weighted fraction meeting a service target is also reported. These summarize

sampled outcomes, rather than field outage probabilities. Approximate 95% intervals for paired service contrasts use stratified sampling variance and a Welch–Satterthwaite Student-t approximation, with the finite-population correction omitted. They describe uncertainty from sampled starts conditional on this annual scenario, not variation across independent years.

Normal operating cost combines grid purchases, assessed BESS wear and settled EV payments. Paired differences distinguish reserve-enabled BESS savings from additional routine EV dispatch. Payments are separated into energy reimbursement, wear reimbursement and owner profit. SOC, credited reserve hours, energy flows, and cycle/calendar wear explain the monetary outcomes; the PWA scheduling cost is not substituted for assessed wear. Outage deployment and owner-profit accounts use Eqs. (48)–(50), including displaced normal operation and signed ending-inventory settlement.

5.5 Frequency and infrastructure boundaries

The solved event library is reused for 0, 0.316, 1, 3, 5, 10, 20, 30, 34, 50 and 100 events/site-year, separately for each evaluated duration. The normal annual saving enters once; only incremental event consequences are scaled by frequency. No traffic-loss price is asserted in the base case. Instead, the break-even account in Eq. (49) identifies which nonnegative service values could cover incremental cost. Signed service differences are retained: an alternative carrying less traffic may have an upper admissible value, or no feasible interval, rather than a positive "minimum required value." The controller's mean-restoration parameter of 1.2317 h and the 0.316 frequency grid point are declared scenarios, not measured BS outage statistics.

Existing compatible infrastructure has zero additional capital cost. New-installation scenarios total 17,300 €, 29,000 € and 50,000 € for four bidirectional ports and site integration. These are cost ranges for screening, not verified supplier quotations. Their annual cost is

$$C_{\mathrm{EVSE}}^{\mathrm{ann}} = C_0 \left[\frac{r_d(1+r_d)^L}{(1+r_d)^L - 1} + \omega_{\mathrm{OM}} \right]. \tag{56}$$

The installed cost is C_0 [€], the real annual discount rate is $r_d = 0.04$, the economic lifetime is $L = 10$ years, and annual maintenance is $\omega_{\mathrm{OM}} = 0.02$ of installed cost. Equal installations cancel between EV-enabled alternatives. These annual charges do not alter short-run dispatch.

Frequency scaling assumes independent events and leaves normal schedules and owner agreements unchanged. It does not simulate recovery limits, successive outages or heatwave clustering. Cases with $fD/8784 > 0.02$ are flagged as outside the selected low-duty screening range, where f is events/year and D is hours/event. The 2% cutoff is a declared screening rule, not a validity theorem; even cases below it retain the independent-event approximation. Long-duration cases carry no inferred occurrence probability. Additional capacity, temperature, enrollment and forecast-error grids were not evaluated; no robustness claim is drawn from those optional settings.

Table 4 Objective-gap certificates for each optimization stage.

Stage	Relative gap	Absolute gap
Normal dispatch	1%	0.01 €
Outage service	0.1%	10^{-5} GB
Outage cost	0.5%	0.005 €

5.6 Numerical checks and evidence scope

MILPs are solved with Gurobi. A feasible incumbent is required, together with either the relative or the absolute objective-gap certificate in Table 4. Outage cost minimization preserves the first-stage service incumbent within 10^{-6} GB, separately from its optimality gap.

The completed run passed its mandatory physical and numerical audits. Actual incumbent values and bounds are recorded. These per-solve gaps do not certify annual global optimality or the precision of small annual profit differences. Physical audits check energy balance, SOC limits, EV floors and connection bounds, reserve compliance during normal operation, inventory closure and prohibited simultaneous charging and discharging. Outage EV-to-BESS transfer is permitted and checked against the outage energy balance. Source and configuration identities, completed path counts and figure-source records support reproducibility. Memory restarts reuse only verified work within the same run identity.

Results support conditional comparisons of the stated policies and assumptions, without establishing cross-year uncertainty, guaranteed availability or universal deployment profitability.

AI-assisted tools. OpenAI ChatGPT was used to assist with software development and review, figure preparation, and manuscript drafting and revision. Responsibility for verifying the model, numerical results, references, and final text rests with the authors.

6 Results and Discussion

The evaluation asks whether connected EVs are more useful as a temporary reserve, as an energy source, or through a combination of these roles. We distinguish the normal-operation savings enabled by reserve sharing from the service delivered during outages and the income received by vehicle owners. The four policies—Standby, EV Backup, EV Reserve, and Joint Dispatch—use the same carrier-aware radio actions during outages, so differences between them arise from storage access and dispatch.

The Italian and Dutch price cases share one annual load and EV realization and 24 sampled outage starts. Means are weighted according to the sampled starts' population shares. The 1-, 2-, 4-, 8-, 16-, and 24-h outcomes are prefixes of common outage trajectories, rather than independent repetitions. Normal scheduling uses the supplied demand path; outage control observes current conditions without knowing

future arrivals or the actual restoration time. The following results therefore describe the evaluated scenario, not measured field reliability.

6.1 EV reserve releases stationary energy before EVs discharge

Figure 3 shows how reserve sharing works in a selected Italian day. Under Standby and EV Backup, the BESS remains at 95% SOC while the grid is available. Under EV Reserve and Joint Dispatch, connected vehicles lower the stationary reserve requirement in proportion to their credited energy. Without EV credit, that requirement returns to the standby level. The BESS supplies the site during a higher-price interval and later recharges before EV reserve expires. The vehicles themselves deliver essentially no energy in this window. Their contribution is nevertheless visible in the stationary SOC and grid-import profiles: they make a different stationary-battery schedule feasible.

At least one enrolled vehicle is connected in 49.25% of the annual intervals in the assumed fleet scenario. Under Joint Dispatch, the BESS operates below the 95% standby level for 34.51% of the year in Italy and 35.33% in the Netherlands. Its mean SOC falls to 82.25% and 80.03%, respectively. The battery need not follow the instantaneous reserve floor: prices, converter limits, departure times, and degradation costs determine how much of the available flexibility is used. Every policy starts and ends the year with 9.5 kWh in the stationary battery, excluding savings obtained by depleting initial inventory.

Table 5 reports annual normal-operation costs, including electricity purchases, modeled battery wear, and owner compensation. EV Backup and Standby have identical normal-operation costs because both preserve stationary standby energy and exclude normal EV dispatch. EV Reserve, which also excludes direct EV discharge while the grid is available, saves 51.17 € in Italy and 109.33 € in the Netherlands, or 2.90% and 8.26% of the respective Standby costs. Joint Dispatch saves 51.43 € and 110.63 €, equivalent to 2.91% and 8.36% of the corresponding standby costs. These are operating savings with existing compatible infrastructure and no fixed availability fee.

Table 5 Annual normal-operation cost and saving relative to Standby [€/site-year].

	Italy		Netherlands	
Policy	Cost	Saving	Cost	Saving
Standby	1764.36	0.00	1324.11	0.00
EV Backup	1764.36	0.00	1324.11	0.00
EV Reserve	1713.19	51.17	1214.78	109.33
Joint Dispatch	1712.93	51.43	1213.48	110.63

The reported additional saving from allowing direct EV dispatch is only 0.26 € in Italy and 1.30 € in the Netherlands. Annual EV discharge at the site bus is 2.99 and

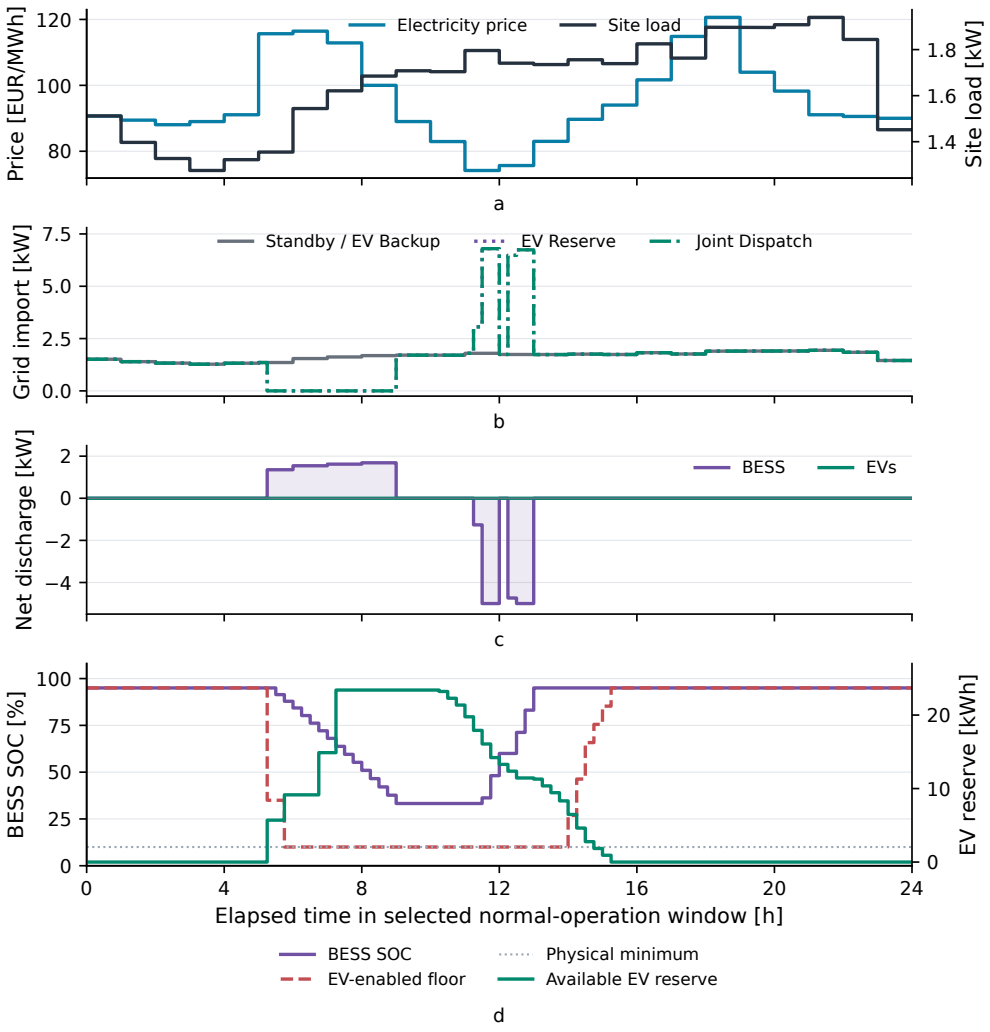


Fig. 3 Selected normal-operation day in Italy: (a) electricity price and site load, (b) grid import, (c) net storage discharge, and (d) BESS SOC and available EV reserve. Negative net discharge denotes charging.

32.58 kWh, compared with 1987.40 and 2303.75 kWh from the BESS. EV Reserve alone therefore captures about 99% of the reported Joint Dispatch saving in each market. The main normal-operation benefit comes from making stationary energy available for economic dispatch, rather than from supplying large amounts of EV energy. These small differences should not be interpreted as a precisely established annual advantage of Joint Dispatch, because the rolling-window solver tolerances do not certify differences of this size.

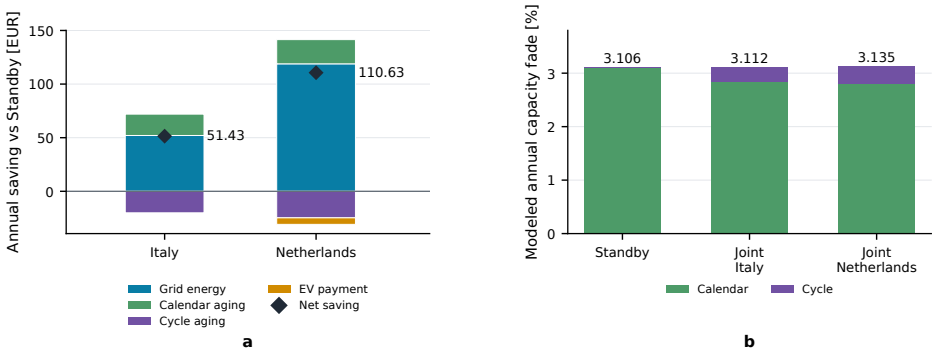


Fig. 4 Joint Dispatch economics and BESS aging: (a) annual saving components relative to Standby, with diamonds marking net savings; (b) modeled calendar and cycle capacity fade.

The Dutch price series makes this flexibility more valuable in the same site scenario. It also allows more direct EV discharge, but this remains a small part of normal-operation energy supply. The comparison does not establish a general price-spread threshold: the value of a price difference also depends on when vehicles connect and whether power and departure constraints permit the site to use it.

6.2 Calendar-aging gains are offset by additional cycling

Figure 4(a) explains the net savings. Under Joint Dispatch, grid expenditure falls by 52.06 € in Italy and 118.87 € in the Netherlands. Lower calendar-aging costs add 19.91 € and 22.59 €, while cycle-aging costs rise by 20.34 € and 24.75 €. EV compensation reduces the remaining saving by 0.20 € and 6.08 €. The reduction in electricity expenditure therefore supports the final saving even though the combined BESS-aging cost increases slightly.

The capacity-fade estimates in Fig. 4(b) show the same trade-off. Calendar fade decreases from 3.106% under Standby to 2.841% in Italy and 2.805% in the Netherlands. Additional cycling raises total modeled fade to 3.112% and 3.135%, slightly above standby. Lower SOC reduces calendar exposure in this model, but cycling offsets that reduction. The result supports a trade-off between the two aging mechanisms, rather than an extension of battery life. These normal-operation estimates also depend on the declared chemistry, temperature, and aging calibration.

Lower expenditure should not be confused with lower electricity use. Annual grid purchases increase by 215.10 kWh in Italy and 243.16 kWh in the Netherlands, consistent with conversion losses from additional storage cycling. The schedules shift purchases towards cheaper intervals; they do not demonstrate reduced total energy consumption or emissions.

6.3 EV support during long outages

During outages, the controller prioritizes carried traffic and then minimizes cost while preserving its first-stage service incumbent. EV energy can therefore be used to protect

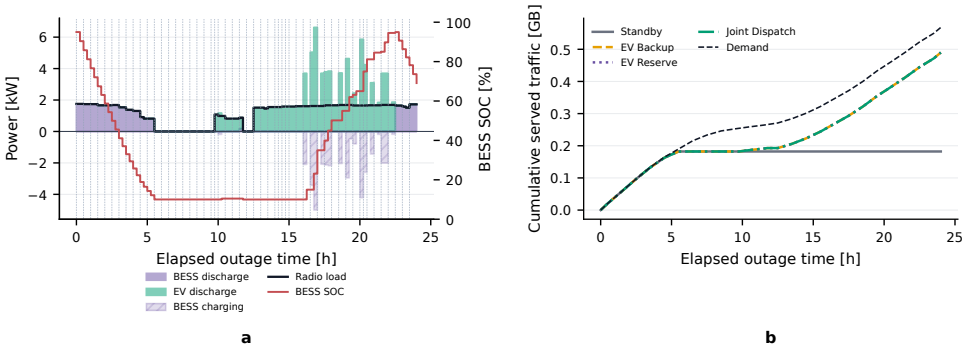


Fig. 5 Selected causal 24-h outage in Italy: (a) Joint Dispatch power flows and BESS SOC; (b) cumulative carried and requested traffic.

service even when direct EV dispatch offers little normal-operation economic benefit. Figure 5 follows one selected 24-h outage in Italy. Stationary energy initially supplies the radio load. As energy becomes scarce, the controller reduces service, and a period without service occurs before further EV energy becomes accessible. Vehicles arriving later enter the plan only after connection. They can then support current demand and recharge the stationary battery, allowing service to resume. This trajectory illustrates how temporary energy can be retained in persistent storage; it does not imply uninterrupted service throughout the event.

The weighted outcomes in Fig. 6(a) show that EV support matters most after stationary energy becomes insufficient. At 8 h, Standby retains 75.42% of requested traffic, compared with 94.59% under Joint Dispatch in Italy and 94.86% under Dutch prices. At 24 h, Standby retains 23.12%, while Joint Dispatch retains 84.44% and 84.50%. The weighted worst-decile mean at 24 h rises from 12.75% to 72.10% and 72.14%, respectively. The similar service outcomes in the two price cases contrast with their different normal-operation savings. This is consistent with the shared equipment and traffic scenario and the service-first outage objective; market prices mainly affect the normal schedule and inherited storage states.

Figure 6(b) shows how often a high traffic target is met, which the mean alone cannot reveal. In Italy, the weighted share of sampled scenarios retaining at least 90% of traffic is 79.01% for Joint Dispatch at 8 h, compared with 33.53% for Standby. At 24 h, this share falls to 25.00% for Joint Dispatch and zero for Standby. The corresponding Joint Dispatch share in the Netherlands is 20.95% at 24 h. Temporary storage substantially improves service, but does not make a high service target attainable in every sampled event. Neither these empirical shares nor the worst-decile means are guarantees of field reliability. The rise in the worst-decile mean between 16 and 24 h can reflect later arrivals and a change in which events form the lower tail, rather than an improvement in every individual outage.

EV Backup offers a useful comparison because it retains the full stationary standby inventory and still permits EV support. Its mean retained traffic at 24 h is 84.76% in both markets, slightly above Joint Dispatch, by approximately 0.32 percentage

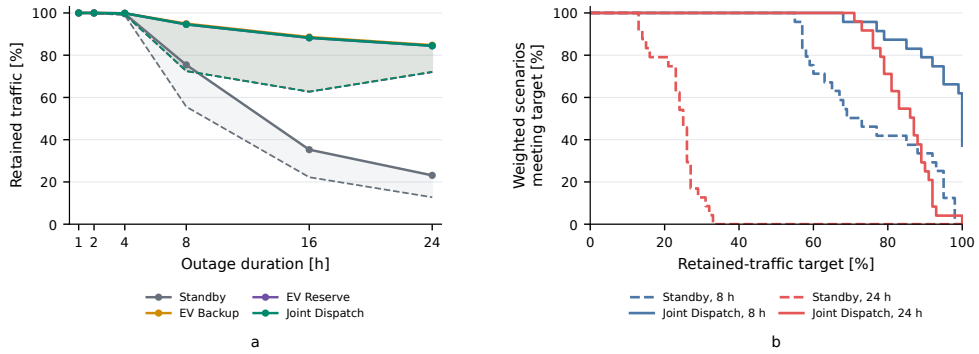


Fig. 6 Outage service in Italy: (a) weighted mean retained traffic (solid) and worst-decile mean (dashed), with shading between them; (b) weighted shares of sampled scenarios meeting traffic targets at 8 and 24 h. Shading is not a confidence interval.

points in Italy and 0.26 in the Netherlands. Reserve sharing provides normal-operation savings, but those savings are accompanied by a small reduction in reported mean service relative to retaining full stationary inventory with EV support. The reserve-only comparison in Table 6 likewise gives slightly lower means for EV Reserve than EV Backup. Its paired intervals include zero; this does not establish equal reliability or non-inferiority.

The matched-state diagnostic isolates EV access from the stationary inventory inherited from normal operation. With the same initial BESS energy in Italy, enabling EV outage support increases retained traffic by 29.35 percentage points at 8 h and 65.48 points at 24 h. These comparisons support the contribution of temporary storage without attributing the gain to a more favorable stationary starting state. The EV-disabled arm is a diagnostic at the reduced BESS inventory, not a stationary-only policy that satisfies the normal standby rule.

6.4 Outage planning improves carried traffic

The one-step benchmark and receding-horizon controller both operate under Joint Dispatch with the same initial resources, feasible radio actions, current observations, and declared departures. Neither sees future EV arrivals, future radio demand, or the realized restoration time. The comparison in Fig. 7 therefore examines planning with the same information, rather than the advantage of knowing when the grid will return.

At 24 h, one-step control retains 58.14% of traffic in Italy and 58.33% in the Netherlands. Receding-horizon control raises these values to 84.44% and 84.50%, gains of 26.30 and 26.16 percentage points. The approximate paired intervals in Table 6 exclude zero for both price cases. The advantage is accompanied by greater resource use: in Italy, mean EV cell-energy withdrawal rises from 15.70 to 25.55 kWh, and event battery/owner cost rises from 5.12 € to 8.42 €. The comparison demonstrates the service benefit of look-ahead under the stated information rules; it does not show that a fixed service level is delivered more cheaply.

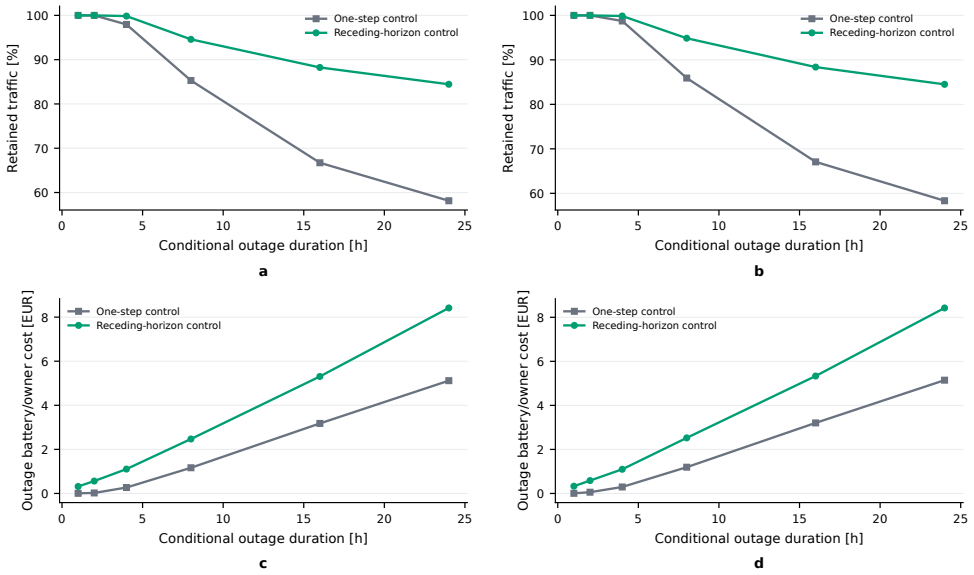


Fig. 7 Outage controller comparison under Joint Dispatch: retained traffic in (a) Italy and (b) the Netherlands, and battery/owner cost in (c) Italy and (d) the Netherlands. Means use 24 common starts with identical initial states and information.

Table 6 Paired retained-traffic differences [percentage points].

Comparison	Italy	Netherlands
EV Backup − Standby (24 h)	61.64 [57.08, 66.19]	61.64 [57.08, 66.19]
EV Reserve − EV Backup (24 h)	−0.31 [−0.76, 0.14]	−0.33 [−0.78, 0.12]
Matched EV support (8 h)	29.35 [20.62, 38.08]	—
Matched EV support (24 h)	65.48 [60.47, 70.49]	—
Receding horizon − one-step (24 h)	26.30 [21.66, 30.94]	26.16 [21.51, 30.82]

Entries give the weighted mean difference and its approximate 95% stratified Student-t interval over 24 common starts, conditional on one annual realization. The first two rows retain policy-specific pre-outage states. Matched EV support compares EV Reserve with an EV-disabled outage controller at the same initial stationary energy and was evaluated only for Italy. The controller comparison starts from identical BESS and EV states. These intervals do not describe variation across independently generated years.

During the 24-h events, EV-to-BESS transfers under Joint Dispatch add a mean 5.59 kWh to stationary cell energy in Italy and 5.66 kWh in the Netherlands, after charging losses. Storing some connected EV energy can preserve its availability after the vehicle leaves, subject to converter losses and battery limits. This illustrates the complementary roles of persistent and departure-limited storage. The observed

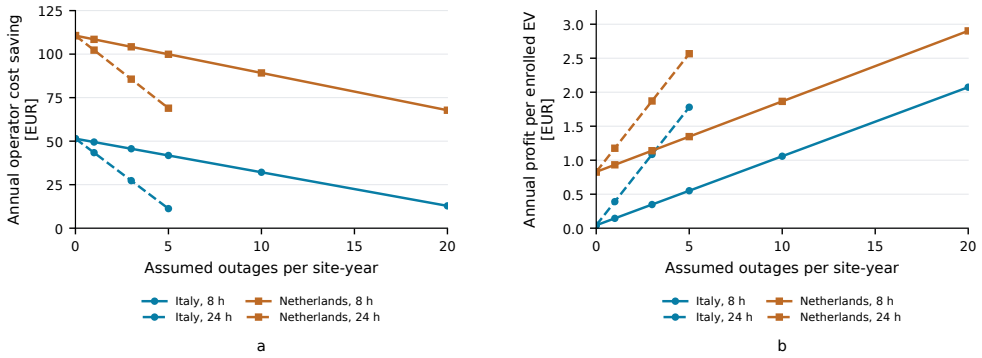


Fig. 8 Independent-event economic screen under Joint Dispatch for 8- and 24-h outages: (a) annual operator cost saving relative to Standby, including modeled battery wear; (b) annual profit per enrolled EV, excluding energy and degradation reimbursements. Only frequency points within the low-duty screening range are shown.

controller gain remains conditional on the declared restoration prior and planning horizon.

6.5 Owner income and operator savings respond differently to outages

Figure 8 combines annual normal-operation accounts with incremental costs and owner profit from the sampled outage events, including the specified inventory settlement. The frequency screen treats events independently; it does not simulate successive failures and recovery. Only supplied frequency points within the declared 2% annual outage-time screening range are shown: up to 20 events per year for 8-h outages and five for 24-h outages. Retained traffic is not assigned a monetary value, and no new bidirectional infrastructure cost is charged in this comparison. The monetary accounts include modeled battery wear, rather than representing measured cash flows.

At five 8-h outages per year, estimated operator cost savings are 41.78 € in Italy and 99.92 € in the Netherlands. Annual profit per enrolled EV is only 0.55 € and 1.35 €. For five 24-h outages, operator savings fall to 11.25 € and 68.94 €, while owner profit rises to 1.78 € and 2.57 €. These owner values exclude energy and degradation reimbursements; they are the participation margin, not total compensation for supplied energy.

In this independent-event screen, increasing outage frequency raises owner income because vehicles are activated more often. Operator cost savings fall because activation costs rise and preserved service has no assigned monetary value. For 24-h outages in Italy, the accounting break-even boundary is approximately 6.40 events per year. This is a boundary of the independent-event calculation, rather than an additional simulated annual trajectory or a point shown in the figure. Beyond it, additional event costs relative to Standby exceed the normal-operation saving. This is a cost-only boundary, not a conclusion that EV support lacks value when avoided service loss is considered.

The owner's limited income and the site's reserve-sharing saving should also be distinguished. Normal-operation owner profit totals 0.17 € in Italy and 3.31 € in the Netherlands across all four enrolled vehicles. Reserve availability receives no fixed payment in the base agreement, so the site's benefit from released BESS reserve is not automatically shared with owners. The reported operating savings therefore rely on assumed enrollment under an agreement with unpaid reserve availability. Positive modeled profit alone does not establish a sufficient incentive to enroll. Applying Eq. (56) to the stated installation scenarios gives annual charges of approximately 2,479–7,165 €/year, exceeding the normal-operation savings in both markets. A dedicated installation would therefore require additional benefits, such as the value of avoided service loss, to cover these costs; that value has not been estimated here.

Taken together, the evaluated scenario supports two distinct EV roles: reserve availability enables normal-operation BESS savings, while actual energy delivery sustains substantially more traffic during long outages. The benefit is conditional on connection timing, the owner agreement and existing compatible infrastructure; it does not establish preserved standby reliability or installation payback. The reported solves meet their declared gap criteria and registered physical and information checks, as described in Section 5.6. These checks concern internal consistency, rather than field validation or global annual optimality.

7 Lessons Learned

EV availability and EV energy delivery have different economic roles. A connected vehicle can help the site even when it does not discharge: its credited reserve allows stationary energy to be used during normal operation. In this experiment, that role accounts for almost all of the saving relative to standby. Direct EV dispatch adds little under the evaluated owner agreement and prices. The practical implication is that reserve availability should be assessed separately from energy delivery. Connection times, power limits and departure requirements determine which price differences the site can use, so the larger saving with Dutch prices does not establish a general price-spread threshold. Lower SOC reduces calendar exposure in the adopted aging model, while additional cycling offsets that gain. Operating cost, energy consumption and battery lifetime therefore need separate assessments.

Reserve sharing also changes the stationary inventory available when a failure begins. Keeping the BESS fully charged with the same EV access gives slightly higher mean retention in the reported 24-h comparison. Reserve sharing should therefore be assessed against the operator's service requirement, rather than assumed to preserve standby reliability. During an outage, departure times and new arrivals determine when EV energy remains accessible. Transferring some of that energy into the BESS can retain it after a vehicle leaves. Receding-horizon planning improves carried traffic without knowing restoration time, but incurs greater battery and owner costs. The relevant trade-off is service delivered against resource use, rather than cost minimization alone.

The participation agreement determines how benefits are divided between the site and vehicle owners. The site benefits from reserve sharing, yet owners receive little

profit when availability is unpaid and compensation follows energy activation. Paying for reserved availability could share some of that value, but would reduce operator savings. Existing compatible infrastructure is central to the reported operating benefit: the stated new-installation costs are not covered by these savings alone. Practical adoption would require a site-specific value for avoided service loss and evidence that owners accept the departure-energy agreement. Successive outages and recovery, unexpected departures, and independently generated fleet years remain outside the present evaluation.

8 Conclusion

This study evaluates whether connected EVs can release stationary backup energy for economic use while also supporting a base station during outages. Without EV reserve credit, the BESS remains at its 95% standby SOC during normal operation. Connected EVs lower that reserve requirement; prices, degradation costs and owner compensation then determine whether the available flexibility is used. Paired policies separate this reserve effect from direct EV dispatch and outage support.

For the evaluated 10-kWh BESS and annual fleet scenario, Joint Dispatch reduces total normal-operation cost by 2.91% under Italian prices and 8.36% under Dutch prices relative to Standby. Almost all of the reported saving is obtained without normal EV discharge. Lower calendar aging is offset by additional cycling, so the experiment does not demonstrate longer battery life. During the sampled 24-h outages, mean retained traffic increases from 23.12% under Standby to 84.44% and 84.50% under Joint Dispatch. Receding-horizon planning gains about 26 percentage points over one-step control with the same initial resources and information.

These outcomes are conditional on one annual scenario and 24 common outage starts per price case. Improved average service does not guarantee a high traffic target in every event. The results identify distinct benefits from EV reserve availability and emergency energy delivery at sites with existing compatible infrastructure; they do not establish new-installation payback or sufficient owner incentives. Further evaluation should use observed participation and restoration records and model successive outages together with recovery.

Abbreviations

Abbreviation	Definition
BS	Base station
BESS	Battery energy storage system
EV	Electric vehicle
EVSE	Electric vehicle supply equipment
V2G	Vehicle-to-grid
MNO	Mobile network operator
SOC	State of charge
MILP	Mixed-integer linear programming
PWA	Piecewise-affine
SOS2	Special ordered set of type 2
LFP	Lithium iron phosphate
NMC	Lithium nickel manganese cobalt oxide
EFC	Equivalent full cycle
LTE	Long Term Evolution
NR	New Radio
UTC	Coordinated Universal Time

Declarations

Ethics approval and consent to participate

Not applicable. The study uses aggregate base-station records and numerical simulations. EV sessions, energy states and enrollment are scenario inputs; no participants were recruited for this study.

Consent for publication

Not applicable.

Availability of data and materials

The public electricity-price source and the simulation assumptions are identified in Section 5. EV sessions in the reported experiment are generated from the declared parametric scenario. The underlying operator traffic trace is subject to confidentiality restrictions and cannot be redistributed publicly. Non-confidential derived inputs, simulation outputs, figure-source tables and the simulation code are available from the corresponding author on reasonable request, subject to source-data permissions.

Competing interests

The authors declare that they have no competing interests.

Funding

No specific funding was received for this work.

Authors' contributions

MRJ developed the methodology and software, performed the analysis and visualization, and prepared the original manuscript draft. GV and DR contributed to the methodology, validation, interpretation of the results and manuscript revision. MM contributed to the conceptualization, supervision, interpretation, project administration and manuscript revision.

Acknowledgements

Not applicable.

References

[1] Wallnerström, C.J., Dalheim, M., Seratelius, M., Johansson, T.: Power outage related statistics in sweden since the early 2000s and evaluation of reliability trends. In: 2020 International Conference on Probabilistic Methods Applied to Power Systems (PMAPS) (2020). https://doi.org/10.1109/PMAPS47429.2020.9183500

[2] Yong, P., Zhang, N., Hou, Q., Liu, Y., Teng, F., Ci, S., Kang, C.: Evaluating the dispatchable capacity of base station backup batteries in distribution networks. IEEE Transactions on Smart Grid **12**(5), 3966–3979 (2021) https://doi.org/10.1109/TSG.2021.3074754

[3] Gholipoor, N., Hamzeh Aghdam, F., Rasti, M., Zarini, H.: Strategic utilization of cellular operator energy storage for smart grid frequency regulation. IEEE Transactions on Smart Grid **16**(5), 3961–3975 (2025) https://doi.org/10.1109/TSG.2025.3581770

[4] Naumann, M., Schimpe, M., Keil, P., Hesse, H.C., Jossen, A.: Analysis and modeling of calendar aging of a commercial LiFePO4/graphite cell. Journal of Energy Storage **17**, 153–169 (2018) https://doi.org/10.1016/j.est.2018.01.019

[5] Collath, N., Cornejo, M., Engwerth, V., Hesse, H.C., Jossen, A.: Increasing the lifetime profitability of battery energy storage systems through aging-aware operation. Applied Energy **348**, 121531 (2023) https://doi.org/10.1016/j.apenergy.2023.121531

[6] Leippi, A., Fleschutz, M., Davis, K., Klingler, A.-L., Murphy, M.D.: Optimizing electric vehicle fleet integration in industrial demand response: Maximizing vehicle-to-grid benefits while compensating vehicle owners for battery degradation. Applied Energy **374**, 123995 (2024) https://doi.org/10.1016/j.apenergy.2024.123995

[7] Sagaria, S., Kam, M., Boström, T.: Vehicle-to-grid impact on battery degradation and estimation of V2G economic compensation. Applied Energy **377**, 124546

(2025) https://doi.org/10.1016/j.apenergy.2024.124546

[8] Jokar, M.R., Vallero, G., Renga, D., Meo, M.: Leveraging on-site EVs for enhanced stationary battery utilization and reliability in base stations. In: 2026 Joint European Conference on Networks and Communications & 6G Summit (EuCNC/6G Summit), Málaga, Spain (2026). https://doi.org/10.1109/EuCNC/6GSummit68295.2026.11577474

[9] European Network of Transmission System Operators for Electricity: ENTSO-E Transparency Platform: Day-Ahead Electricity Prices. Online data platform. Accessed 25 September 2026 (2024). https://transparency.entsoe.eu/

[10] Bont, K., Hoogsteen, G., Hurink, J.L., Kokhuis, R., Kusche, F., Nijenhuis, B., Özceylan, B., Ruijter, J., Schubbel, A., Velden, J., Winschermann, L., Zweistra, M.: Electric Vehicle Charging Session Data of Large Office Parking Lot. 4TU.ResearchData (2024). https://doi.org/10.4121/80ef3824-3f5d-4e45-8794-3b8791efbd13

[11] Cabrera-Tobar, A., Vallero, G., Perin, G., Meo, M., Grimaccia, F., Leva, S.: Adaptive energy management system for green and reliable telecommunication base stations. Energies **18**(23), 6115 (2025) https://doi.org/10.3390/en18236115

[12] Zheng, F., Chen, K., Liu, M.: Optimization of communication base station battery configuration considering demand transfer and sleep mechanism under uncertain interruption duration. Sustainability **15**(24), 16645 (2023) https://doi.org/10.3390/su152416645

[13] Xu, B., Zhao, J., Zheng, T., Litvinov, E., Kirschen, D.S.: Factoring the cycle aging cost of batteries participating in electricity markets. IEEE Transactions on Power Systems **33**(2), 2248–2259 (2018) https://doi.org/10.1109/TPWRS.2017.2733339

[14] Truong, V.B., Le, L.B.: Building energy management and electric vehicle charging considering battery degradation and random vehicles' arrivals and departures. Journal of Energy Storage **64**, 107141 (2023) https://doi.org/10.1016/j.est.2023.107141

[15] Thrän, J., Mareček, J., Shorten, R.N., Green, T.C.: Reserve provision from electric vehicles: Aggregate boundaries and stochastic model predictive control. IEEE Transactions on Power Systems **40**(5), 4081–4092 (2025) https://doi.org/10.1109/TPWRS.2025.3539863

[16] Ayaz, F., Nekovee, M., Sheng, Z., Saeed, N.: Digital twin-based reinforcement learning for energy exchange among electric vehicles and base stations in a disaster-affected region. IEEE Transactions on Intelligent Transportation Systems **27**(5), 6181–6190 (2026) https://doi.org/10.1109/TITS.2025.3607305

[17] Auer, G., Giannini, V., Desset, C., Gödör, I., Skillermark, P., Olsson, M., Imran, M.A., Sabella, D., Gonzalez, M.J., Blume, O., Fehske, A.: How much energy is needed to run a wireless network? IEEE Wireless Communications **18**(5), 40–49 (2011) https://doi.org/10.1109/MWC.2011.6056691

[18] Vallero, G., Pristeri, E., Meo, M.: Coping with power outages in mobile networks. In: 2020 Mediterranean Communication and Computer Networking Conference (MedComNet), pp. 1–4 (2020). https://doi.org/10.1109/MedComNet49392.2020.9191585

[19] Naumann, M., Spingler, F.B., Jossen, A.: Analysis and modeling of cycle aging of a commercial LiFePO4/graphite cell. Journal of Power Sources **451**, 227666 (2020) https://doi.org/10.1016/j.jpowsour.2019.227666

[20] National Renewable Energy Laboratory: BLAST-Lite: Battery Lifetime Analysis and Simulation Tool–Lite. Open-source software. Accessed 5 October 2026; supplied calendar input table identifies version 1.1.1 (2023). https://github.com/NatLabRockies/BLAST-Lite